

Measurement of the Bottom contribution to non-photon electron production in $p + p$ collisions at $\sqrt{s}=200$ GeV

M. M. Aggarwal,³¹ Z. Ahammed,²² A. V. Alakhverdyants,¹⁸ I. Alekseev,¹⁶ J. Alford,¹⁹ B. D. Anderson,¹⁹ Daniel Anson,²⁹ D. Arkhipkin,³ G. S. Averichev,¹⁸ J. Balewski,²³ L. S. Barnby,² S. Baumgart,⁵³ D. R. Beavis,³ R. Bellwied,⁵¹ M. J. Betancourt,²³ R. R. Betts,⁸ A. Bhasin,¹⁷ A. K. Bhati,³¹ H. Bichsel,⁵⁰ J. Bielcik,¹⁰ J. Bielcikova,¹¹ B. Biritz,⁶ L. C. Bland,³ B. E. Bonner,³⁷ J. Bouchet,¹⁹ E. Braidot,²⁸ A. V. Brandin,²⁶ A. Bridgeman,¹ E. Bruna,⁵³ S. Bueltmann,³⁰ I. Bunzarov,¹⁸ T. P. Burton,³ X. Z. Cai,⁴¹ H. Caines,⁵³ M. Calderón de la Barca Sánchez,⁵ O. Catu,⁵³ D. Cebra,⁵ R. Cendejas,⁶ M. C. Cervantes,⁴³ Z. Chajecki,²⁹ P. Chaloupka,¹¹ S. Chattopadhyay,⁴⁸ H. F. Chen,³⁹ J. H. Chen,⁴¹ J. Y. Chen,⁵² J. Cheng,⁴⁵ M. Cherney,⁹ A. Chikanian,⁵³ K. E. Choi,³⁵ W. Christie,³ P. Chung,¹¹ R. F. Clarke,⁴³ M. J. M. Codrington,⁴³ R. Corliss,²³ J. G. Cramer,⁵⁰ H. J. Crawford,⁴ D. Das,⁵ S. Dash,¹³ A. Davila Leyva,⁴⁴ L. C. De Silva,⁵¹ R. R. Debbe,³ T. G. Dedovich,¹⁸ A. A. Derevschikov,³³ R. Derradi de Souza,⁷ L. Didenko,³ P. Djawotho,⁴³ S. M. Dogra,¹⁷ X. Dong,²² J. L. Drachenberg,⁴³ J. E. Draper,⁵ J. C. Dunlop,³ M. R. Dutta Mazumdar,⁴⁸ L. G. Efimov,¹⁸ E. Elhalhuli,² M. Elnimr,⁵¹ J. Engelage,⁴ G. Eppley,³⁷ B. Erasmus,⁴² M. Estienne,⁴² L. Eun,³² O. Evdokimov,⁸ P. Fachini,³ R. Fatemi,²⁰ J. Fedorisin,¹⁸ R. G. Fersch,²⁰ P. Filip,¹⁸ E. Finch,⁵³ V. Fine,³ Y. Fisyak,³ C. A. Gagliardi,⁴³ D. R. Gangadharan,⁶ M. S. Ganti,⁴⁸ E. J. Garcia-Solis,⁸ A. Geromitsos,⁴² F. Geurts,³⁷ V. Ghazikhanian,⁶ P. Ghosh,⁴⁸ Y. N. Gorbunov,⁹ A. Gordon,³ O. Grebenyuk,²² D. Grosnick,⁴⁷ S. M. Guertin,⁶ A. Gupta,¹⁷ W. Guryn,³ B. Haag,⁵ A. Hamed,⁴³ L-X. Han,⁴¹ J. W. Harris,⁵³ J. P. Hays-Wehle,²³ M. Heinz,⁵³ S. Heppelmann,³² A. Hirsch,³⁴ E. Hjort,²² A. M. Hoffman,²³ G. W. Hoffmann,⁴⁴ D. J. Hofman,⁸ B. Huang,³⁹ H. Z. Huang,⁶ T. J. Humanic,²⁹ L. Huo,⁴³ G. Igo,⁶ P. Jacobs,²² W. W. Jacobs,¹⁵ C. Jena,¹³ F. Jin,⁴¹ C. L. Jones,²³ P. G. Jones,² J. Joseph,¹⁹ E. G. Judd,⁴ S. Kabana,⁴² K. Kajimoto,⁴⁴ K. Kang,⁴⁵ J. Kapitan,¹¹ K. Kauder,⁸ D. Keane,¹⁹ A. Kechechyan,¹⁸ D. Kettler,⁵⁰ D. P. Kikola,²² J. Kiryluk,²² A. Kisiel,⁴⁹ V. Kizka,¹⁸ S. R. Klein,²² A. G. Knospe,⁵³ A. Kocoloski,²³ D. D. Koetke,⁴⁷ T. Kollegger,¹² J. Konzer,³⁴ I. Koralt,³⁰ L. Koroleva,¹⁶ W. Korsch,²⁰ L. Kotchenda,²⁶ V. Kouchpil,¹¹ P. Kravtsov,²⁶ K. Krueger,¹ M. Krus,¹⁰ L. Kumar,¹⁹ P. Kurnadi,⁶ M. A. C. Lamont,³ J. M. Landgraf,³ S. LaPointe,⁵¹ J. Lauret,³ A. Lebedev,³ R. Lednicky,¹⁸ C-H. Lee,³⁵ J. H. Lee,³ W. Leight,²³ M. J. LeVine,³ C. Li,³⁹ L. Li,⁴⁴ N. Li,⁵² W. Li,⁴¹ X. Li,³⁴ X. Li,⁴⁰ Y. Li,⁴⁵ Z. M. Li,⁵² G. Lin,⁵³ X. Y. Lin,⁵² S. J. Lindenbaum,²⁷ M. A. Lisa,²⁹ F. Liu,⁵² H. Liu,⁵ J. Liu,³⁷ T. Ljubicic,³ W. J. Llope,³⁷ R. S. Longacre,³ W. A. Love,³ Y. Lu,³⁹ E. V. Lukashov,²⁶ X. Luo,³⁹ G. L. Ma,⁴¹ Y. G. Ma,⁴¹ D. P. Mahapatra,¹³ R. Majka,⁵³ O. I. Mall,⁵ L. K. Mangotra,¹⁷ R. Manweiler,⁴⁷ S. Margetis,¹⁹ C. Markert,⁴⁴ H. Masui,²² H. S. Matis,²² Yu. A. Matulenko,³³ D. McDonald,³⁷ T. S. McShane,⁹ A. Meschanin,³³ R. Milner,²³ N. G. Minaev,³³ S. Mioduszewski,⁴³ A. Mischke,²⁸ M. K. Mitrovski,¹² B. Mohanty,⁴⁸ M. M. Mondal,⁴⁸ B. Morozov,¹⁶ D. A. Morozov,³³ M. G. Munhoz,³⁸ B. K. Nandi,¹⁴ C. Nattrass,⁵³ T. K. Nayak,⁴⁸ J. M. Nelson,² P. K. Netrakanti,³⁴ M. J. Ng,⁴ L. V. Nogach,³³ S. B. Nurushev,³³ G. Odyniec,²² A. Ogawa,³ V. Okorokov,²⁶ E. W. Oldag,⁴⁴ D. Olson,²² M. Pachr,¹⁰ B. S. Page,¹⁵ S. K. Pal,⁴⁸ Y. Pandit,¹⁹ Y. Panebratsev,¹⁸ T. Pawlak,⁴⁹ T. Peitzmann,²⁸ V. Perevoztchikov,³ C. Perkins,⁴ W. Peryt,⁴⁹ S. C. Phatak,¹³ P. Pile,³ M. Planinic,⁵⁴ M. A. Ploskon,²² J. Pluta,⁴⁹ D. Plyku,³⁰ N. Poljak,⁵⁴ A. M. Poskanzer,²² B. V. K. S. Potukuchi,¹⁷ C. B. Powell,²² D. Prindle,⁵⁰ C. Pruneau,⁵¹ N. K. Pruthi,³¹ P. R. Pujahari,¹⁴ J. Putschke,⁵³ H. Qiu,²¹ R. Raniwala,³⁶ S. Raniwala,³⁶ R. L. Ray,⁴⁴ R. Redwine,²³ R. Reed,⁵ H. G. Ritter,²² J. B. Roberts,³⁷ O. V. Rogachevskiy,¹⁸ J. L. Romero,⁵ A. Rose,²² C. Roy,⁴² L. Ruan,³ R. Sahoo,⁴² S. Sakai,⁶ I. Sakrejda,²² T. Sakuma,²³ S. Salur,⁵ J. Sandweiss,⁵³ E. Sangaline,⁵ J. Schambach,⁴⁴ R. P. Scharenberg,³⁴ N. Schmitz,²⁴ T. R. Schuster,¹² J. Seele,²³ J. Seger,⁹ I. Selyuzhenkov,¹⁵ P. Seyboth,²⁴ E. Shalahiev,¹⁸ M. Shao,³⁹ M. Sharma,⁵¹ S. S. Shi,⁵² E. P. Sichtermann,²² F. Simon,²⁴ R. N. Singaraju,⁴⁸ M. J. Skoby,³⁴ N. Smirnov,⁵³ P. Sorensen,³ J. Sowinski,¹⁵ H. M. Spinka,¹ B. Srivastava,³⁴ T. D. S. Stanislaus,⁴⁷ D. Staszak,⁶ J. R. Stevens,¹⁵ R. Stock,¹² M. Strikhanov,²⁶ B. Stringfellow,³⁴ A. A. P. Suaide,³⁸ M. C. Suarez,⁸ N. L. Subba,¹⁹ M. Sumner,¹¹ X. M. Sun,²² Y. Sun,³⁹ Z. Sun,²¹ B. Surrow,²³ D. N. Svirida,¹⁶ T. J. M. Symons,²² A. Szanto de Toledo,³⁸ J. Takahashi,⁷ A. H. Tang,³ Z. Tang,³⁹ L. H. Tarini,⁵¹ T. Tarnowsky,²⁵ D. Thein,⁴⁴ J. H. Thomas,²² J. Tian,⁴¹ A. R. Timmins,⁵¹ S. Timoshenko,²⁶ D. Tlusty,¹¹ M. Tokarev,¹⁸ T. A. Trainor,⁵⁰ V. N. Tram,²² S. Trentalange,⁶ R. E. Tribble,⁴³ O. D. Tsai,⁶ J. Ulery,³⁴ T. Ullrich,³ D. G. Underwood,¹ G. Van Buren,³ M. van Leeuwen,²⁸ G. van Nieuwenhuizen,²³ J. A. Vanfossen, Jr.,¹⁹ R. Varma,¹⁴ G. M. S. Vasconcelos,⁷ A. N. Vasiliev,³³ F. Videbaek,³ Y. P. Vijoyi,⁴⁸ S. Vokal,¹⁸ S. A. Voloshin,⁵¹ M. Wada,⁴⁴ M. Walker,²³ F. Wang,³⁴ G. Wang,⁶ H. Wang,²⁵ J. S. Wang,²¹

Q. Wang,³⁴ X. L. Wang,³⁹ Y. Wang,⁴⁵ G. Webb,²⁰ J. C. Webb,³ G. D. Westfall,²⁵ C. Whitten Jr.,⁶ H. Wieman,²²
 S. W. Wissink,¹⁵ R. Witt,⁴⁶ Y. F. Wu,⁵² W. Xie,³⁴ H. Xu,²¹ N. Xu,²² Q. H. Xu,⁴⁰ W. Xu,⁶ Y. Xu,³⁹
 Z. Xu,³ L. Xue,⁴¹ Y. Yang,²¹ P. Yepes,³⁷ K. Yip,³ I-K. Yoo,³⁵ Q. Yue,⁴⁵ M. Zawisza,⁴⁹ H. Zbroszczyk,⁴⁹
 W. Zhan,²¹ J. B. Zhang,⁵² S. Zhang,⁴¹ W. M. Zhang,¹⁹ X. P. Zhang,²² Y. Zhang,²² Z. P. Zhang,³⁹ J. Zhao,⁴¹
 C. Zhong,⁴¹ J. Zhou,³⁷ W. Zhou,⁴⁰ X. Zhu,⁴⁵ Y. H. Zhu,⁴¹ R. Zoukarnееv,¹⁸ and Y. Zoukarnееva¹⁸

(STAR Collaboration)

- ¹Argonne National Laboratory, Argonne, Illinois 60439, USA
²University of Birmingham, Birmingham, United Kingdom
³Brookhaven National Laboratory, Upton, New York 11973, USA
⁴University of California, Berkeley, California 94720, USA
⁵University of California, Davis, California 95616, USA
⁶University of California, Los Angeles, California 90095, USA
⁷Universidade Estadual de Campinas, Sao Paulo, Brazil
⁸University of Illinois at Chicago, Chicago, Illinois 60607, USA
⁹Creighton University, Omaha, Nebraska 68178, USA
¹⁰Czech Technical University in Prague, FNSPE, Prague, 115 19, Czech Republic
¹¹Nuclear Physics Institute AS CR, 250 68 Řež/Prague, Czech Republic
¹²University of Frankfurt, Frankfurt, Germany
¹³Institute of Physics, Bhubaneswar 751005, India
¹⁴Indian Institute of Technology, Mumbai, India
¹⁵Indiana University, Bloomington, Indiana 47408, USA
¹⁶Alikhanov Institute for Theoretical and Experimental Physics, Moscow, Russia
¹⁷University of Jammu, Jammu 180001, India
¹⁸Joint Institute for Nuclear Research, Dubna, 141 980, Russia
¹⁹Kent State University, Kent, Ohio 44242, USA
²⁰University of Kentucky, Lexington, Kentucky, 40506-0055, USA
²¹Institute of Modern Physics, Lanzhou, China
²²Lawrence Berkeley National Laboratory, Berkeley, California 94720, USA
²³Massachusetts Institute of Technology, Cambridge, MA 02139-4307, USA
²⁴Max-Planck-Institut für Physik, Munich, Germany
²⁵Michigan State University, East Lansing, Michigan 48824, USA
²⁶Moscow Engineering Physics Institute, Moscow Russia
²⁷City College of New York, New York City, New York 10031, USA
²⁸NIKHEF and Utrecht University, Amsterdam, The Netherlands
²⁹Ohio State University, Columbus, Ohio 43210, USA
³⁰Old Dominion University, Norfolk, VA, 23529, USA
³¹Panjab University, Chandigarh 160014, India
³²Pennsylvania State University, University Park, Pennsylvania 16802, USA
³³Institute of High Energy Physics, Protvino, Russia
³⁴Purdue University, West Lafayette, Indiana 47907, USA
³⁵Pusan National University, Pusan, Republic of Korea
³⁶University of Rajasthan, Jaipur 302004, India
³⁷Rice University, Houston, Texas 77251, USA
³⁸Universidade de Sao Paulo, Sao Paulo, Brazil
³⁹University of Science & Technology of China, Hefei 230026, China
⁴⁰Shandong University, Jinan, Shandong 250100, China
⁴¹Shanghai Institute of Applied Physics, Shanghai 201800, China
⁴²SUBATECH, Nantes, France
⁴³Texas A&M University, College Station, Texas 77843, USA
⁴⁴University of Texas, Austin, Texas 78712, USA
⁴⁵Tsinghua University, Beijing 100084, China
⁴⁶United States Naval Academy, Annapolis, MD 21402, USA
⁴⁷Valparaiso University, Valparaiso, Indiana 46383, USA
⁴⁸Variable Energy Cyclotron Centre, Kolkata 700064, India
⁴⁹Warsaw University of Technology, Warsaw, Poland
⁵⁰University of Washington, Seattle, Washington 98195, USA
⁵¹Wayne State University, Detroit, Michigan 48201, USA
⁵²Institute of Particle Physics, CCNU (HZNU), Wuhan 430079, China
⁵³Yale University, New Haven, Connecticut 06520, USA
⁵⁴University of Zagreb, Zagreb, HR-10002, Croatia
- (Dated: October 27, 2018)

The contribution of B meson decays to non-photonic electrons, which are mainly produced by the semi-leptonic decays of heavy flavor mesons, in $p + p$ collisions at $\sqrt{s} = 200$ GeV has been measured using azimuthal correlations between non-photonic electrons and hadrons. The extracted B decay contribution is approximately 50% at a transverse momentum of $p_T \geq 5$ GeV/ c . These measurements constrain the nuclear modification factor for electrons from B and D meson decays. The result indicates that B meson production in heavy ion collisions is also suppressed at high p_T .

PACS numbers: 25.75.-q

The suppression of non-photonic electron yields from semi-leptonic decays of D and B mesons for p_T up to 9 GeV/ c in central Au+Au collisions at Relativistic Heavy Ion Collider (RHIC) has been observed to be large [1], and similar to that of light quark hadrons [2]. Due to the dead cone effect, heavy quarks were expected to lose less energy than light quarks [3] if the dominant energy loss mechanism is gluon radiation [4]. Various models have been proposed to explain the large suppression of non-photonic electron yields [5–7]. Theoretical calculations of the non-photonic electron suppression crucially depend on the B/D ratios because the amount of radiative energy loss depends on the quark mass. Measuring the bottom quark contribution to non-photonic electron yields in $p + p$ collisions is therefore important in order to understand the production of heavy quarks and to provide a baseline for the energy loss measurement of heavy quarks in the hot and dense medium produced in central Au+Au collisions.

In this paper, we report a determination of the relative contribution from B decays to non-photonic electron yields (r_B) by measuring the azimuthal correlations between non-photonic electrons and charged hadrons ($e_{\text{non}\gamma}\text{-}h$), and between non-photonic electrons and D^0 mesons ($e_{\text{non}\gamma}\text{-}D^0$) in $p + p$ collisions at $\sqrt{s} = 200$ GeV by the STAR experiment at RHIC. We fit the experimental $e_{\text{non}\gamma}\text{-}h$ correlations using a combination of PYTHIA calculations [8] for D and B meson decays and extract r_B as a function of p_T ($2.5 < p_T < 9.5$ GeV/ c). An independent measurement of the r_B is obtained from $e_{\text{non}\gamma}\text{-}D^0$ correlations, by selecting the charge combinations $e^- \text{-} D^0 (\rightarrow K^-)$ and $e^+ \text{-} \bar{D}^0 (\rightarrow K^+)$, which provide relatively pure samples of B decays and charm pairs on near and away-side ($\Delta\phi \sim \pi$) [9]. The combined measurements of the B decay contribution and of the nuclear modification factor (R_{AA}) for heavy-flavor decay electrons in Au+Au collisions constrain the value of the R_{AA} for electrons from B meson decays.

The $p + p$ data used in this analysis were taken by the STAR experiment [10] during the 2005 and 2006 RHIC runs. The main detectors for this analysis are the Time Projection Chamber (TPC) and the Barrel Electromagnetic Calorimeter (BEMC). The BEMC has a Shower Maximum Detector (SMD): proportional gas chambers with strip readout at a depth of ~ 5 radiation lengths (X_0) designed to measure shower shapes and positions. The acceptance for electrons in pseudorapidity and az-

imuth is $|\eta| < 0.7$ ($0 < \eta < 0.7$ in the 2005 run) and $0 < \phi < 2\pi$. The BEMC also serves as a trigger detector for high p_T electrons or photons, where single-tower transverse energy thresholds of 2.6 GeV and 5.4 GeV were used. The total sampled luminosity was 11.3 pb^{-1} (0.65 pb^{-1}) for the 5.4 GeV (2.6 GeV) trigger threshold. We used triggered events with primary vertices located within 35 cm of the TPC's geometrical center along the beam direction.

Electrons were identified by measuring ionization energy loss (dE/dx) and track momentum (p) from TPC, the energy (E) deposition in the BEMC, and the shower profile in the SMD. A significant fraction of the hadron background was rejected by selecting tracks with a measured dE/dx in the TPC between -1 and $+3$ standard deviations from the expected mean dE/dx for electrons. Based on calibrations of the SMD response to electrons and hadrons, tracks whose shower projection occupies more than 1 strip in both ϕ and η SMD planes were selected as electron candidates. We required the energy-to-momentum ratio to be in the range $0.3 < p/E < 1.5$. The hadron contamination in the electron sample after applying these cuts is $\sim 2\%$ up to 5 GeV/ c , increasing to $\sim 10\%$ at 9 GeV/ c .

The electron sample has two components: (1) non-photonic electrons and (2) photonic electrons - those from photon conversion in the detector material between the interaction point and the TPC and Dalitz decays, mainly from π^0 . Photonic electrons were identified by pairing electrons with oppositely charged partner tracks, determining the conversion or decay vertex, and calculating the invariant mass of the e^+e^- pair $M_{e^+e^-}$ [11]. To improve the invariant mass resolution, the so-called 2-D invariant mass was calculated using only p_T and p_Z , which is equivalent to setting the opening angle in the transverse plane to zero [11]. Monte Carlo simulations indicate that the cut of $0.1 \text{ GeV}/c^2$ removes almost all photon conversion candidates for which the decay partner is reconstructed in the TPC. The efficiencies for photonic electron reconstruction (ϵ_{e_γ}) range from 65% at 3.0 GeV/ c to 80% at 8.0 GeV/ c , as determined from GEANT simulations. For the $e_{\text{non}\gamma}\text{-}h$ analysis, we first removed the electrons that have an opposite-sign partner such that $M_{e^+e^-} < 0.1 \text{ GeV}/c^2$ from the inclusive electron sample. The remaining electrons form the ‘‘semi-inclusive’’ electron sample. The non-photonic electron yields can be

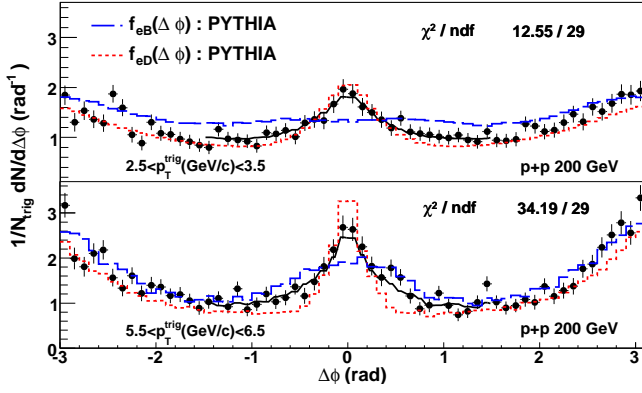


FIG. 1: (color online) Distributions of the azimuthal angle between non-photonic electrons and charged hadrons normalized per non-photonic electron trigger. The trigger electron has (top) $2.5 < p_T < 3.5$ GeV/c and (bottom) $5.5 < p_T < 6.5$ GeV/c. The curves represent PYTHIA calculations for D (dotted curve) and B (dashed curve) decays. The fit result is shown as the black solid curve.

expressed as,

$$N_{e_{\text{non}\gamma}} = N_{e_{\text{semi}}} + N_{e_{\text{like}}} - N_{e_{\text{not-reco}}} - N_h. \quad (1)$$

$N_{e_{\text{semi}}}$ is the number of semi-inclusive electrons. $N_{e_{\text{not-reco}}}$ represents the number of photonic electrons which are not reconstructed by the invariant mass method and is defined as: $(1/\epsilon_{e_\gamma} - 1)(N_{e_{\text{unlike}}} - N_{e_{\text{like}}})$. $N_{e_{\text{like}}}$ is the number of non-photonic electrons that were rejected by the conversion cuts because they happened to form a pair with a random track which is determined using like-sign pairs. N_h is the remaining background from hadron contamination in the electron sample. Other weak decay contributions such as K_{e3} are negligible due to their long $c\tau$, and charmed baryons (mostly Λ_c) is expected to be very small contribution since the baryon yield is small compared to the meson yield ($\Lambda_c/D^0 \sim 0.1$ in PYTHIA) and the branching ratio for semi-leptonic decays is smaller for baryons than mesons. The $e_{\text{non}\gamma}$ - h azimuthal distributions were calculated as

$$\begin{aligned} \frac{dN_{e_{\text{non}\gamma-h}}}{d(\Delta\phi)} &= \frac{dN_{e_{\text{semi-h}}}}{d(\Delta\phi)} + \frac{dN_{e_{\text{like-h}}}}{d(\Delta\phi)} - \frac{dN_{e_{\text{not-reco-h}}}}{d(\Delta\phi)} \\ &\quad - \frac{dN_{h-h}}{d(\Delta\phi)}, \end{aligned} \quad (2)$$

where each term is normalised to be per non-photonic electron trigger. Each angle-difference distribution on the right-hand side of Eq. (2) was experimentally determined. The distribution $dN_{e_{\text{not-reco-h}}}/d(\Delta\phi)$ was constructed from $dN_{e_{\text{reco-h}}}/d(\Delta\phi)$ by removing the conversion partner to account for the fact that the partner electron is not reconstructed.

Figure 1 shows $dN_{e_{\text{non}\gamma-h}}/d(\Delta\phi)$ per trigger for non-photonic electrons for two different trigger p_T selections.

Associated particles were required to have $p_T > 0.3$ GeV/c and $|\eta| < 1.05$. The dotted (dashed) line in the figure represents a PYTHIA version 6.22 calculation of the azimuthal correlations between electrons from D (B) meson decay and charged hadrons ($f_{eD}(\Delta\phi)$, $f_{eB}(\Delta\phi)$) [12]. PYTHIA was tuned to reproduce the shapes of p_T distributions for D mesons measured by STAR [12, 13]. The PYTHIA calculation shows that the near-side peak for $f_{eB}(\Delta\phi)$ is broader than that for $f_{eD}(\Delta\phi)$. These shapes are dominated by decay kinematics. The fragmentation function does not affect the shape in a significant way. The fraction of non-photonic electrons from B meson decay can be determined by fitting the near-side distribution function ($|\Delta\phi| < 1.5$):

$$\frac{1}{N_{\text{trig}}^{\text{non}\gamma}} \frac{dN_{e_{\text{non}\gamma-h}}}{d(\Delta\phi)} = r_B f_{eB}(\Delta\phi) + (1 - r_B) f_{eD}(\Delta\phi), \quad (3)$$

where r_B is the ratio of electrons from B meson decay to the total non-photonic electron yield, $r_B = N_{eB}/(N_{eB} + N_{eD}) = N_{eB}/N_{e_{\text{non}\gamma}}$.

An independent measurement of r_B was performed using $e_{\text{non}\gamma}$ - D^0 correlations. D^0 mesons were reconstructed via their hadronic decay $D^0 \rightarrow K^-\pi^+$ ($\mathcal{B} = 3.89\%$) by calculating the invariant mass of all oppositely charged TPC tracks in the same event. In this analysis, only events with a non-photonic electron trigger were used for D^0 reconstruction. Furthermore, the kaon candidates were required to have the same charge sign as the non-photonic electrons [9]. The combinatorial background of random pairs was evaluated by combining all charged tracks with the same charge sign from the same event. The requirement of a non-photonic electron trigger suppresses the combinatorial background, yielding a signal (S)-to-background (B) ratio of about 14% and a signal significance ($S/\sqrt{S+B}$) of ~ 4.6 .

Figure 2 (a) shows the background subtracted π - K invariant mass distribution. The peak position and width were determined using a Gaussian fit to the data. The $K\pi$ invariant mass distribution was obtained for different $\Delta\phi$ bins with respect to the trigger electron, and the yield of the associated D^0 mesons was taken as the area underneath the Gaussian fit to the signal. Figure 2 (b) shows the azimuthal correlation of $e_{\text{non}\gamma}$ - D^0 , which exhibits near- and away-side correlation peaks with similar yields. The results are fitted with the correlation functions for charm and bottom production from PYTHIA and MC@NLO simulations having the relative B contribution as a free parameter [9]. The observed away-side correlation peak can be attributed to prompt charm pair production ($\sim 75\%$) and B decays ($\sim 25\%$), whereas the contributions to the near-side peak are mainly from B decays. We determined r_B by fitting the measured $e_{\text{non}\gamma}$ - D^0 correlation with PYTHIA and MC@NLO and used the average of the two fits for the final value.

Figure 3 shows $r_B = N_{eB}/(N_{eB} + N_{eD})$ extracted from $e_{\text{non}\gamma}$ - h correlations (filled circles) and $e_{\text{non}\gamma}$ - D^0 corre-

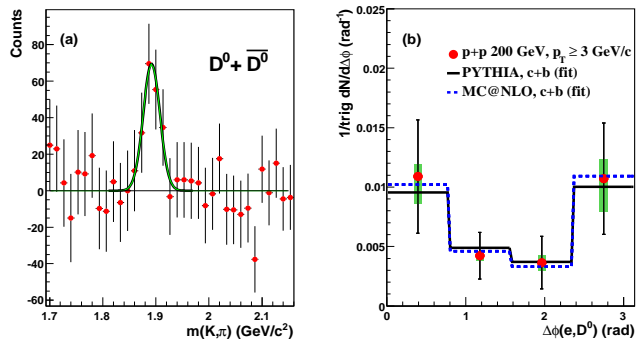


FIG. 2: (a) Background-subtracted invariant mass distribution of $K\pi$ pairs requiring at least one non-photonic electron trigger in the event. The solid line is a Gaussian fit to the data near the peak region. (b) Distribution of the azimuthal angle between non-photonic electron (positron) trigger particles and D^0 (\bar{D}^0). The solid (dashed) line is a fit of the correlation function from PYTHIA (MC@NLO) simulations to the data points.

lations (open circle) as a function of p_T . The vertical lines represent the statistical errors and the systematic uncertainties are shown as brackets. The systematic uncertainties due to electron identification ($\sim 7\%$), photonic electron rejection ($\sim 6\%$), the fit range ($\sim 10\%$) and the normalization of the azimuthal distribution ($\sim 10\%$), PYTHIA and MC@NLO predictions for $e_{non\gamma} - D^0$ ($\sim 5\%$), and the D^0 signal extraction were estimated by varying the associated cut parameters and adding the individual contributions in quadrature. r_B increases with electron p_T and reaches approximately 0.5 ($N_{e_B}/N_{e_D} \sim 1$) around $p_T = 5$ GeV/c. r_B from the $e_{non\gamma} - D^0$ correlation measurement at $p_T \sim 5.5$ GeV/c is consistent with r_B from $e_{non\gamma} - h$ correlations. The curve in the figure is r_B from a FONLL pQCD calculation including theoretical uncertainties [14]. Similar ratios at $2 < p_T < 7$ GeV/c using a different method have also been reported [15]. J/ψ di-electron decays can also contribute to non-photonic electrons and STAR measurement of J/ψ at high p_T indicates that J/ψ decays could contribute nearly 10% around p_T 5 GeV/c. The estimated effect of the electrons from J/ψ decays on r_B is a few percent, much smaller than the current statistical and systematic uncertainties, and no correction was applied to our data.

Next, we explore the implications of the measured r_B for the R_{AA} of electrons from B meson decay in heavy ion collisions. The R_{AA} for heavy flavor non-photonic electrons (R_{AA}^{HF}) is given by

$$R_{AA}^{HF} = (1 - r_B)R_{AA}^{eD} + r_B R_{AA}^{eB}, \quad (4)$$

where R_{AA}^{eD} (R_{AA}^{eB}) is the R_{AA} for electrons from D (B) mesons. From Eq. (4), R_{AA}^{eD} and R_{AA}^{eB} are related by the B decay contribution to the non-photonic electron

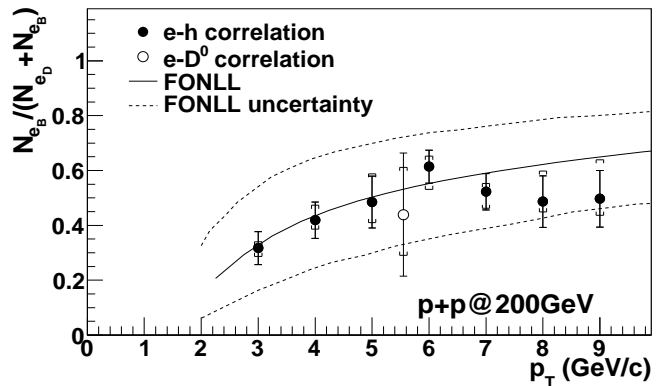


FIG. 3: Transverse momentum dependence of the relative contribution from B mesons (r_B) to the non-photonic electron yields. Error bars are statistical and brackets are systematic uncertainties. The solid curve is the FONLL calculation [14]. Theoretical uncertainties are indicated by the dashed curves.

yields (r_B) in $p + p$ collisions. We have taken the R_{AA}^{HF} measurement from PHENIX [16, 17] and fit the R_{AA}^{HF} above $p_T > 5$ GeV/c to a constant value and obtained: $R_{AA} = 0.167_{-0.0485}^{+0.0562}$ (stat) $_{-0.0815}^{+0.0512}$ (syst) ± 0.0117 (norm), where the statistical and systematic errors are evaluated from weighted average over these $p_T > 5$ GeV/c points. We also calculate the weighted mean r_B value for $p_T > 5$ GeV/c including statistical and systematic errors from our measurement: $r_B = 0.54 \pm 0.0349$ (sta.) ± 0.0666 (sys.). Then using Eq. 4 we calculate a likelihood distribution for R_{AA}^{eB} as a function of R_{AA}^{eD} and the results are shown in Fig. 4. The most probable values for the R_{AA}^{eD} and R_{AA}^{eB} correlation are shown by the line with open circles and the 90% Confidence Limit curves are represented by dashed lines. This result indicates that B meson yields are suppressed at high p_T in heavy ion collisions presumably due to energy loss of the b quark in the dense medium [5] or of the heavy flavor hadrons due to dissociation [6] or elastic scattering [7]. Our conclusion does not change if we use the R_{AA} measurement from [1] and ignore the J/ψ feeddown contributions.

For comparison, we also show model calculations in Fig. 4. Model I includes radiative energy loss via a few hard scatterings with initial gluon density $dN_g/dy = 1000$ [5]. Model II includes cold nuclear matter effects, partonic energy loss and collisional dissociation [6]. Model III assumes a large elastic scattering cross section associated with resonance states of D and B mesons in the QGP [7]. The model contours in Fig. 4 are calculated from the p_T dependences of R_{AA} for D and B decay in the interval $5 < p_T \lesssim 9$ GeV/c. For model I and II, the uncertainties are also taken into account. The experimental results are consistent with models II and III but are incompatible with model I. Recently AdS/CFT the-

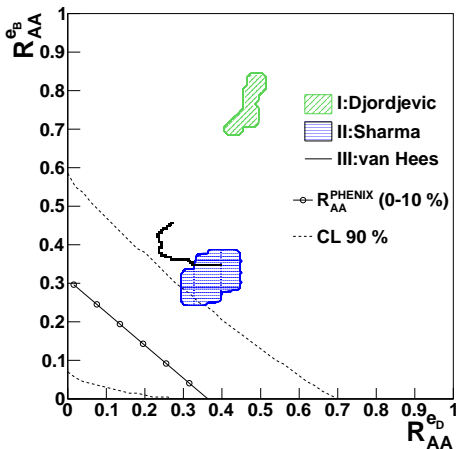


FIG. 4: (color online) Confidence level contours for nuclear modification factor R_{AA} for electrons from D (R_{AA}^{eD}) and B (R_{AA}^{eB}) meson decays and determined by combining the R_{AA} results and the r_B measurement for $p_T > 5$ GeV/c. Three different models of R_{AA} for D and B are described in the text.

ory has also been used to calculate the heavy quark energy loss in a strongly coupled quark-gluon plasma matter, for example [18, 19]. The theory also predicts strong suppressions for charm and bottom, and the ratio of the nuclear modification factors is proposed to differentiate AdS/CFT calculation from others [20].

In summary, we measured the relative contribution from B decays to the non-photonic electron production in $p+p$ collisions at $\sqrt{s} = 200$ GeV by using azimuthal correlations between non-photonic electrons and hadrons (h , D^0). Our result indicates that the B decay contribution increases with p_T and is comparable to the contribution from D meson decay at $p_T \geq 5$ GeV/c. Our measurement is consistent with the FONLL calculation. The ratio of $N_{eB}/(N_{eD} + N_{eB})$ combined with the large suppression of non-photonic electrons indicates that R_{AA} for electrons from B hadron decays is significantly smaller than unity and therefore B meson production is suppressed at high p_T in heavy ion collisions. The constraint on R_{AA}^{eD} and R_{AA}^{eB} will help to differentiate theoretical model calculations for heavy quark energy loss in the dense medium.

We thank the RHIC Operations Group and RCF at BNL, the NERSC Center at LBNL and the Open Sci-

ence Grid consortium for providing resources and support. This work was supported in part by the Offices of NP and HEP within the U.S. DOE Office of Science, the U.S. NSF, the Sloan Foundation, the DFG cluster of excellence ‘Origin and Structure of the Universe’ of Germany, CNRS/IN2P3, STFC and EPSRC of the United Kingdom, FAPESP CNPq of Brazil, Ministry of Ed. and Sci. of the Russian Federation, NNSFC, CAS, MoST, and MoE of China, GA and MSMT of the Czech Republic, FOM and NWO of the Netherlands, DAE, DST, and CSIR of India, Polish Ministry of Sci. and Higher Ed., Korea Research Foundation, Ministry of Sci., Ed. and Sports of the Rep. Of Croatia, Russian Ministry of Sci. and Tech, and RosAtom of Russia.

-
- [1] A. Adare *et al.*, Phys. Rev. Lett. **98**, 172301 (2007).
 - [2] J. Adams *et al.*, Phys. Rev. Lett. **91**, 172302 (2003).
 - [3] Yu. L. Dokshitzer and D. E. Kharzeev, Phys. Lett. B **519**, 199 (2001).
 - [4] M. Gyulassy and M. Plumer, Phys. Lett. B **243**, 432 (1990).
 - [5] M. Djordjevic, M. Gyulassy, R. Vogt, S. Wicks, Phys. Lett. B **632**, 81 (2006).
 - [6] R. Sharma, I. Vitev and Ben-Wei Zhang, Phys. Rev. C **80**, 054902 (2009).
 - [7] H. van Hees, V. Greco and R. Rapp, Phys. Rev. C **73**, 034913 (2006) and private communication.
 - [8] T. Sjöstrand, Comput. Phys. Commun. **135**, 238 (2001).
 - [9] A. Mischke, Phys. Lett. B **671**, 361 (2009).
 - [10] K. H. Ackermann *et al.*, Nucl. Instr. Meth. A **499**, 624 (2003).
 - [11] J. Adams *et al.*, Phys. Rev. C **70**, 044902 (2004).
 - [12] X. Lin, arXiv:hep-ph/0602067.
 - [13] J. Adams *et al.*, Phys. Rev. Lett. **94**, 062301 (2005).
 - [14] M. Cacciari, P. Nason and R. Vogt, Phys. Rev. Lett. **95**, 122001 (2005).
 - [15] A. Adare *et al.*, Phys. Rev. Lett. **103**, 082002 (2009).
 - [16] A. Adare *et al.*, arXiv:1005.1627.
 - [17] We found a mistake in the published data in Phys. Rev. Lett. **98**, 192301 (2007). An erratum is in preparation.
 - [18] S. S. Gubser, Phys. Rev. D **74**, 126005 (2006).
 - [19] C. P. Herzog *et al.*, JHEP **0607** 013 (2006).
 - [20] W. A. Horowitz and M. Gyulassy, Phys. Lett. B **666**, 320 (2008).